ACS SyntheticBiology

Research Article

pubs.acs.org/synthbio

Engineering Monoterpene Production in Yeast Using a Synthetic Dominant Negative Geranyl Diphosphate Synthase

Codruta Ignea,[†] Marianna Pontini,[†,‡] Massimo E. Maffei,[‡] Antonios M. Makris,[§] and Sotirios C. Kampranis[†,∥,*]

[†]Mediterranean Agronomic Institute of Chania, P.O. Box 85, Chania 73100, Greece

[‡]Plant Physiology Unit, Department of Plant Biology, Innovation Centre, University of Turin, Via Quarello 11/A, 10135, Turin, Italy

[§]Institute of Applied Biosciences − Centre for Research and Technology Hellas (INAB-CERTH), P.O. Box 60361, Thermi 57001, Thessaloniki, Greece

[∥]Department of Biochemistry, School of Medicine, University of Crete, P.O. Box 2208, Heraklion 71003, Greece

Supporting Information

ABSTRACT: Monoterpenes have an established use in the food and cosmetic industries and have recently also found application as advanced biofuels. Although metabolic engineering efforts have so far achieved significant yields of larger terpenes, monoterpene productivity is lagging behind. Here, we set out to establish a monoterpene-specific production platform in *Saccharomyces cerevisiae* and identified the sequential reaction mechanism of the yeast farnesyl diphosphate synthase Erg20p to be an important factor limiting monoterpene yield. To overcome this hurdle, we engineered Erg20p into a geranyl diphosphate synthase and achieved a significant increase in monoterpene titers. To further improve production, we converted the engineered geranyl diphosphate synthase into a dominant negative form, so as to decrease the ability of the endogenous Erg20p to function as a farnesyl diphosphate synthase, without entirely abolishing sterol biosynthesis. Fusion of the synthetic dominant negative Erg20p variant with the terpene synthase, combined with yeast strain engineering, further improved monoterpene yields and achieved an overall 340-fold increase in sabinene yield over the starting strain. The design described here can be readily incorporated to any dedicated yeast strain, while the developed plasmid vectors and heterozygous ERG20 deletion yeast strain can also be used as a plug-and-play system for enzyme characterization and monoterpene pathway elucidation.

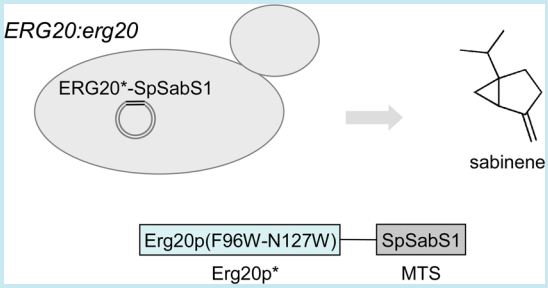

KEYWORDS: *isoprenoid, yeast, protein engineering, farnesyl diphosphate, terpene synthase*

Monoterpenes have long been valued for their fragrance and used as additives in the food and cosmetics industries (e.g., menthol, geraniol, linalool, etc.). Recently, monoterpenes have received increased attention due to their potential application as advanced biofuels. The bicyclic reduced monoterpenes pinane, carane, and sabinane are good candidates for jet air fuel additives, since blends of these monoterpenes with Jet-A1 fuel exhibit improved characteristics.[1] Moreover, mixtures of reduced monoterpene hydrocarbons with farnesane can serve as drop-in jet fuels[2] and have successfully met performance requirements in a demonstration flight.[3]

Basic monoterpene scaffolds contain 10 carbon atoms and are produced by the conversion of geranyl diphosphate (GPP) by a terpene synthase[4] (Figure 1). GPP is formed by condensation of dimethylallyl diphosphate (DMAPP) with its isomer isopentenyl diphosphate (IPP). Addition of one more IPP molecule to GPP gives rise to farnesyl diphosphate (FPP), the precursor of the 15-carbon containing sesquiterpenes (Figure 1). FPP is the substrate for the biosynthesis of sesquiterpenes or geranylgeranyl diphosphate (the precursor of diterpenes), dimerizes to squalene in the first dedicated step in the biosynthesis of sterols, serves as the base molecule in the formation of dolichols, and provides the substrate for the farnesylation of numerous proteins (Figure 1). In yeast and animals, FPP synthesis is catalyzed by a single enzyme that supports the sequential 1′-4 coupling of IPP with DMAPP and GPP. In yeast, this enzyme is Erg20p. Deletion of *ERG20* is lethal,[5] since mutants are unable to synthesize ergosterol,[6] the precursor of vitamin D2 and an essential component of cell membranes required to maintain membrane permeability and fluidity. The biological function of Erg20p may not be limited to FPP synthesis, as it is found to interact with several transcription factors and regulatory molecules (Yta7p, Hir3p, Srb4p and Hap1p,[7] Ssm4p and Aus1p,[8] Sui1p and Prp6p[9]), suggesting possible additional roles of Erg20p both in the cytoplasm and the nucleus.

There is increasing interest in developing biotechnological methods to produce terpenes more economically, sustainably, and in greater quantities than those obtained by extraction from

Received: August 21, 2013
Published: December 24, 2013

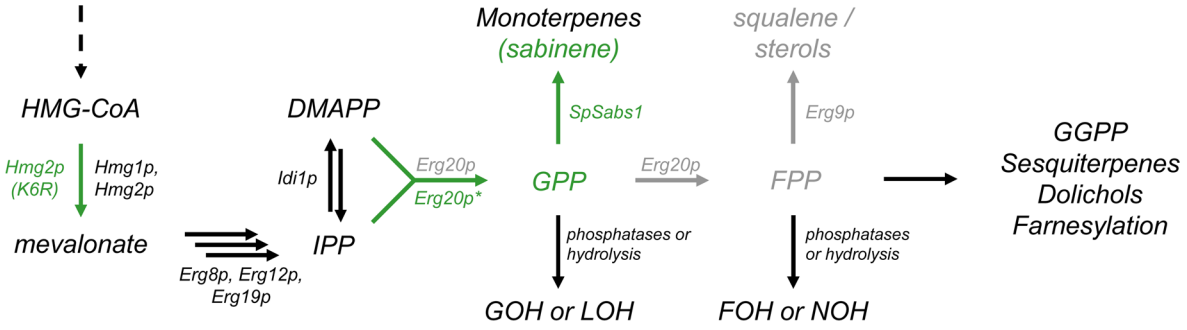

Figure 1. Schematic overview of terpene biosynthesis in yeast indicating the modifications introduced. Upregulated products and pathway steps, or ectopically expressed genes, are indicated in green; downregulated steps or products are in gray. Erg20p variants and fusions are denoted collectively as Erg20p*. (GOH, geraniol; LOH, linalool; FOH, farnesol; NOH, nerolidol).

Table 1. List of *S. cerevisiae* Strains Used

strain	genotype	source
AM78	Mat α, PGal1-*HMG2*(K6R):: HO, *ura3, trp1, his3, leu2*:: PGal1-*IDI1*	24
AM94	Mat a/α, PGal1-*HMG2*(K6R):: HOX2, *ura3, trp1, his3,* P_{TDH3}-*HMG2*(K6R)::*leu2X2*, ERG9/*erg9*	16
AM97	Mat a/α, P_{Gal1}-*HMG2*(K6R):: HOX2, *ura3, trp1, his3,* P_{TDH3}-*HMG2*(K6R)::*leu2X2*, *ERG9/erg9, UBC7/ubc7*. Derived from AM94.	16
AM102	Mat a/α, PGal1-*HMG2*(K6R):: HOX2, *ura3, trp1, his3,* PTDH3-*HMG2*(K6R)*X2*-::*leu2 ERG9/erg9, UBC7/ubc7, SSM4/ssm4*. Derived from AM97.	16
AM109	Mat a/α, PGal1-*HMG2*(K6R):: HOX2, *ura3, trp1, his3,* PTDH3-*HMG2*(K6R)*X2*-::*leu2 ERG9/erg9, UBC7/ubc7, SSM4/ssm4, PHO86/pho86*. Derived from AM102.	16
AM111	Mat a/α, PGal1-*HMG2*(K6R):: HOX2, *ura3, trp1, his3,* PTDH3-*HMG2*(K6R)*X2*-::*leu2 ERG9/erg9, UBC7/ubc7, SSM4/ssm4, PHO86/pho86, lpp1/LPP1*. Derived from AM109.	this study
AM112	Mat a/α, PGal1-*HMG2*(K6R):: HOX2, *ura3, trp1, his3,* PTDH3-*HMG2*(K6R)*X2*-::*leu2 ERG9/erg9, UBC7/ubc7, SSM4/ssm4, PHO86/pho86, dpp1/DPP1*. Derived from AM109.	this study
AM118	Mat a/α, PGal1-*HMG2*(K6R):: HOX2, *ura3, trp1, his3,* PTDH3-*HMG2*(K6R)*X2*-::*leu2 ERG9/erg9, UBC7/ubc7, SSM4/ssm4, PHO86/pho86, dpp1/DPP1, lpp1*/LPP1. Derived from AM112.	this study
MIC2	Mat a/α, PGal1-*HMG2*(K6R):: HOX2, *ura3, trp1, his3,* PTDH3-*HMG2*(K6R)*X2*-::*leu2 ERG9/erg9, ERG20/erg20*. Derived from AM94.	this study

plants or from chemical synthesis. To this end, in recent years there has been significant progress in the metabolic engineering of microorganisms, mainly *Escherichia coli* or *Saccharomyces cerevisiae*. The yeast *S. cerevisiae* in particular is an advantageous host for terpene production due to its robustness, its compatibility with current infrastructure, and the availability of established molecular tools for genetic engineering. Following success in the production of artemisinin in engineered yeast,[10−12] several other terpenes can now be produced in significant amounts in this microorganism. These mainly include the sesquiterpenes bisabolene,[13] epi-aristolochene,[14] santalene,[15] and caryophyllene.[16] Despite achieving significant product yields in efforts focused on sesquiterpenes, the efficiency of monoterpene production in yeast has so far been significantly lower.[17,18] With growing interest in the biotechnological application of monoterpenes, either as fuel additives and drop-in fuel, or as sustainable alternatives to chemically synthesized molecules, we set out to develop a dedicated *S. cerevisiae* platform for the production of monoterpenes. Using a combination of protein and genetic engineering, we modulated prenyl diphosphate levels and achieved a 340-fold increase in monoterpene production over the base strain.

RESULTS AND DISCUSSION

The Sequential Mechanism of FPP Synthesis by Erg20p Hinders Efficient Monoterpene Synthesis. To develop a platform for the efficient production of monoterpenes, the diploid strain AM94[16] was selected as chassis. AM94 contains 3 chromosomally integrated copies of a degradation-stabilized variant of *HMG2* (bearing a K6 to R mutation) and a monoallelic deletion of *ERG9* (Table 1). These modifications minimize product-induced proteolytic degradation of Hmg2p (feedback inhibition) and, at the same time, reduce FPP drain toward sterol biosynthesis.[19] Many terpene synthases produce a range of different products (catalytic promiscuity[20]), thus limiting their suitability for certain biotechnological applications. To set up this platform, we selected the sabinene synthase from *Salvia pomifera* (SpSabS1) due to its high product specificity (~94% sabinene[21]) and the industrial relevance of its main product.[1]

The SpSabS1 ORF was subcloned into the yeast galactose-inducible expression vector pYES2 and introduced into strain AM94. Upon galactose induction, production of sabinene from AM94 cells reached 0.05 mg/L of culture. When the same strain (AM94) was tested for the production of sesquiterpenes by expressing the *S. fruticosa* caryophyllene synthase (SfCarS1[16]), the yield was almost 200 times higher, reaching ~9 mg caryophyllene/L culture. Analysis of the culture extract of AM94 cells expressing SpSabS1 (or containing the empty pYES2 vector) revealed the presence of significant levels of nerolidol (NOH) and farnesol (FOH) (Figure 2A). On the contrary, FOH and NOH levels in the culture medium of SfCarS1-expressing cells were markedly lower (Figure 2A). FOH detected in yeast culture media is formed via hydrolysis of excess FPP by intracellular phosphatases, such as Lpp1p and Dpp1p,[22] while NOH is likely the product of acid hydrolysis of FPP released from the cells.[23] In SfCarS1-expressing cells, the low levels of sesquiterpenols (FOH and NOH) observed can be interpreted as the result of efficient drain of the FPP pool by

dx.doi.org/10.1021/sb400115e | *ACS Synth. Biol.* 2014, 3, 298−306

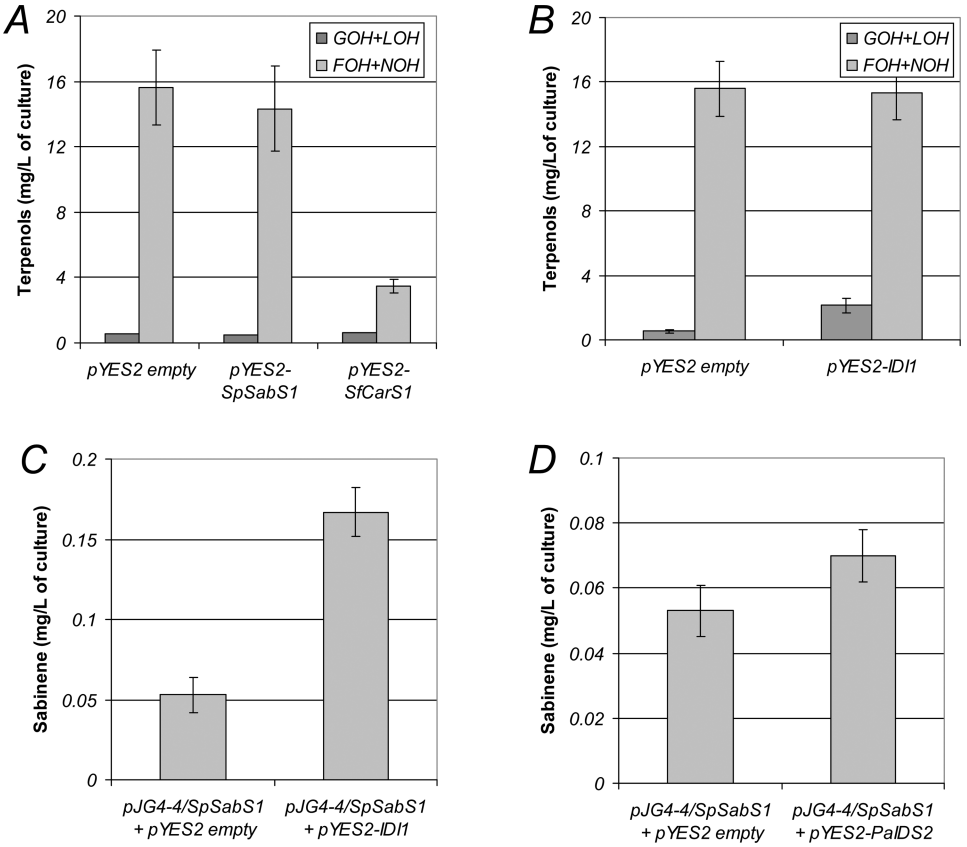

Figure 2. Production of terpenes vs terpenols in yeast cells. (A) Levels of terpenols in AM94 yeast cells expressing *S. pomifera* sabinene synthase (*Sp*SabS1) and *S. fruticosa* caryophyllene synthase (*Sf* CarS1) from the galactose inducible vector pYES2. As described in the text, excess GPP and FPP is released into the medium as GOH and LOH or FOH and NOH, respectively. (B) Expression of IDI1 in AM94 cells enhances the level of GOH and LOH, indicating an increase in the endogenous GPP pool. (C) Coexpression of *Sp*SabS1 (from vector pJG4−4) with IDI1 (from vector pYES2) in AM94 cells increases sabinene production by 3-fold. (D) Coexpression of *P. abies* geranyl diphosphate synthase (*Pa*IDS2) with *Sp*SabS1 in yeast strain AM94 leads to a 40% increase in sabinene yield.

SfCarS1, allowing for only a small fraction of FPP to be converted to NOH or FOH. On the contrary, in SpSabS1 (or empty vector cells), it appears that the terpene synthase cannot efficiently utilize the GPP substrate produced, thus allowing for excess FPP to build up, leading to sesquiterpenol formation. Direct determination of FPP in empty vector and SfCarS1-expressing AM94 cells revealed that the ratio of intracellular FPP between these two strains was similar to the ratio of sesquiterpenols measured in the medium of the above two strains (Supporting Information, Figure S1), suggesting that the amounts of prenyl alcohols detected in the medium can serve as an indirect indicator of the levels of prenyl diphosphates produced by the yeast cells. Under the same conditions, geraniol (GOH) and linalool (LOH) concentrations in the medium of all of the above strains were significantly lower in comparison to the concentrations of sesquiterpenols (Figure 2A). By analogy to FOH and NOH, GOH and LOH are likely also the result of phosphatase or acid hydrolysis of GPP.[18] We measured the ratio of (LOH+GOH)/(NOH+FOH) in AM94 cells to be ∼1:30 (Figure 2A), suggesting that the concentration of intracellular GPP is significantly lower than that of FPP. Indeed, direct measurements of the GPP/FPP ratio in these cells was very similar to the (LOH+GOH)/(NOH+FOH) ratio in the medium (Supporting Information, Figure S2).

Taken together, these observations suggest that inefficient monoterpene synthesis in AM94 is likely due to the low levels of GPP available. This marked difference between the levels of FPP and GPP can be explained on the basis of the sequential mechanism of FPP synthesis by Erg20p, which initially condenses DMAPP with IPP to produce GPP and then adds IPP to GPP to yield FPP (Figure 1). This is in agreement with previous results in which overexpression of isopentenyl diphosphate isomerase (IDI1) in strain AM78 (Table 1) resulted in a 3-fold increase in monoterpene production.[24] Idi1p increases the DMAPP pool at the expense of IPP (Figure 1). This favors the first step of the Erg20p reaction, that of GPP formation, since under these conditions Erg20p is loaded with DMAPP more frequently, leading to a higher GPP/FPP ratio. We overproduced Idi1p in AM94 cells and measured the mono- and sesqui-terpenol levels. Higher levels of Idi1p resulted in a 4-fold increase in the (LOH+GOH)/(NOH +FOH) ratio (Figure 2B), followed by a 3-fold increase in sabinene production (Figure 2C), suggesting that the efficiency of monoterpene production is indeed limited by the levels of the GPP pool.

Conversion of Erg20p into a GPP Synthase. To bypass the limitation posed in monoterpene production by the sequential mechanism of Erg20p, we overexpressed the *Picea abies* GPP synthase (PaIDS2[25]) from a high copy number yeast expression vector, aiming to compete out the second step of the Erg20p reaction and to increase the intracellular GPP concentration. However, only a small increase (30−40%) in sabinene was obtained (Figure 2D). This could be due to poor

dx.doi.org/10.1021/sb400115e | *ACS Synth. Biol.* 2014, 3, 298−306

translation or mRNA stability of PaIDS2 or SpSabS1, protein degradation, improper subcellular localization, or inability of the plant enzymes to associate with relevant yeast multienzymatic complexes. To overcome such potential problems, which are frequently associated with the expression of enzymes in heterologous systems, we opted to convert Erg20p into a GPP synthase by protein engineering. Pioneering work by Poulter and co-workers on the avian FPP synthase (FPS1) identified structural determinants of prenyl chain length control in this enzyme.[26,27] We modeled Erg20p on the structure of FPS1[28] and observed that there is very good conservation in most residues lining the active site cavity despite the evolutionary distance between the yeast and the chicken enzyme. Through a comparison of the Erg20p model with structures of substrate-bound forms of FPS1 (PDB ID: 1UBX, 1UBY), and with the insight provided by the FPS1 mutagenesis studies,[27] we searched for mutations that would hinder the FPP synthase activity of Erg20p without affecting the synthesis of GPP from DMAPP. Two Erg20p residues were identified, F96 and A99 (corresponding to F113 and A116 of FPS1, respectively), which if replaced by a larger side chain could block part of the active site cavity (Figure 3A). F96 of Erg20p was mutated to W, while A99 was mutated to W, F, L, or C. The mutant forms were introduced to an inducible *ERG20*-expressing vector and tested in AM94 cells using sabinene production as the readout. Mutation of A99 to C resulted in only marginal increases in sabinene production, the A99L and A99F mutations improved production by 45% and 70% respectively, and the A99W mutation improved production by almost 2-fold (Figure 3B and Table 2). Mutation of F96 to W had an even stronger effect, improving monoterpene production by 3-fold (Figure 3B and Table 2). Erg20p(F96W) was produced in *E. coli*, purified by affinity chromatography, and its state−state kinetic parameters were determined. The mutant was found to have 30-fold lower affinity for GPP, but only a 2-fold higher K_M for DMAPP, compared to wild-type Erg20p (Table 3), indicating that the observed improvement in monoterpene production in yeast is likely due to its GPP synthase function. These findings also confirm that overexpression of an engineered GPP synthase based on Erg20p has significant advantages over the introduction of an exogenous synthase, presumably due to the limitations discussed.

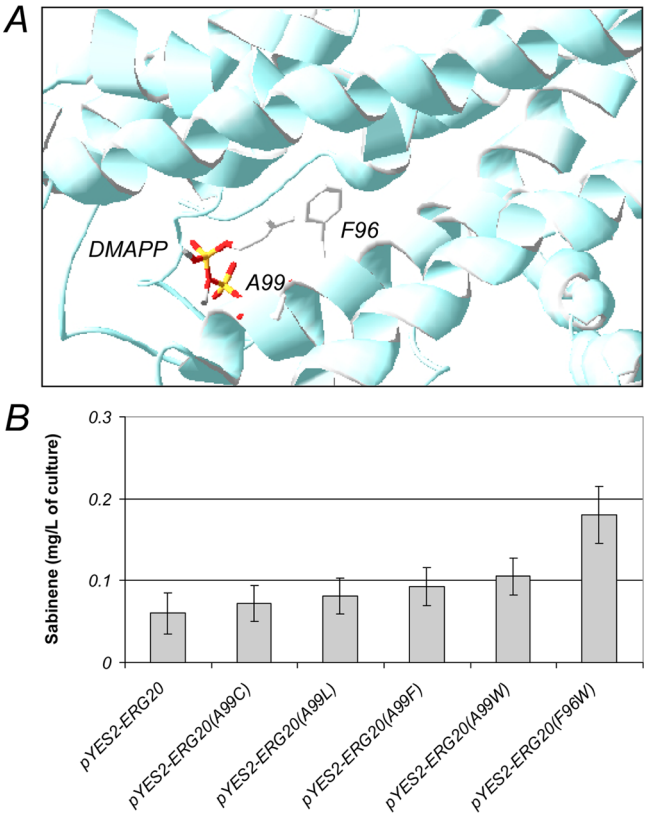

Figure 3. Engineering Erg20p into a geranyl diphosphate synthase and the effect of Erg20p variants on sabinene production. (A) Model of Erg20p showing the residues selected for mutagenesis (F96 and A99). Graphic produced by DeepView (Swiss-PdbViewer). (B) Production of sabinene in yeast cells coexpressing *Sp*SabS1 with different ERG20 mutants. Mutation of F96 to W improves sabinene yield by 3-fold.

Construction of a Dominant Negative Synthase. Examination of the sesquiterpenol levels of Erg20p(F96W)-expressing AM94 cells (or their ability to produce caryophyllene upon introduction of SfCarS1) revealed that these cells are equally capable of producing NOH and FOH (or caryophyllene) as their wild-type Erg20p overexpressing counterparts, indicating that FPP levels are not significantly affected by the introduction of the Erg20p(F96W) mutant, in spite of the increase in monoterpene production (data not shown). This suggests that despite increasing the intracellular GPP levels, the wild-type Erg20p present is sufficient to convert most GPP into FPP. In order to obtain higher titers of monoterpenes, it would be necessary to decrease the concentration of the endogenous enzyme to a level that is sufficiently low so as to reduce competition with the monoterpene synthase for GPP but adequate to provide enough FPP to maintain sterol synthesis, which is essential for cell viability. In the studies of Poulter and co-workers on chicken FPS1, a residue from one subunit of the FPS1 dimer in the crystal form, N144′, was reported to form part of the active site of the other subunit, and its conversion to W abolished FPP (but not GPP) synthesis *in vitro*.[27] Examination of the Erg20p model revealed that N127 of Erg20p is located in a position similar to that of N144′ in the FPS1 structure (Figure 4A). Provided that Erg20p also forms dimers, replacing N127 with a larger side chain may block part of the active site of the opposite subunit and thus enable the mutant protein to function as a dominant negative component, reducing the FPP synthase activity of the endogenous protein. We subcloned the *ERG20* gene into the yeast two-hybrid bait and pray vectors (pGILDA and pJG4−5 respectively) and confirmed that, in EGY48 cells, Erg20p proteins indeed interact (Supporting Information, Figure S3). We subsequently introduced the N127W mutation to pYES2-ERG20 and tested AM94 cells for sabinene production. A 6-fold improvement in yield could be observed (Figure 4B and Table 2), confirming that efficient monoterpene production requires reduction of the endogenous FPP synthase activity.

When the Erg20p(N127W) mutant is present in a homodimeric complex with another Erg20p(N127W) subunit, both subunits would function as a GPP synthase. In a heterodimer with wild-type Erg20p, the Erg20p(N127W) subunit will function as an FPP synthase, while the wild-type subunit as a GPP synthase. To achieve a more efficient reduction of the FPP-synthesizing capacity of the cells, the F96W mutation was introduced into the Erg20p(N127W) protein. The F96W mutation will reduce the ability of the Erg20p(N127W) subunit to function as an FPP synthase in the context of a heterodimer with Erg20p(wt), leaving only

dx.doi.org/10.1021/sb400115e | *ACS Synth. Biol.* 2014, 3, 298−306

Table 2. Overview of Yield Improvement

strain	protein expressed	yield (mg/L of culture)	fold improvement (from previous step)	fold improvement (total)
AM94	SpSabS1	0.051 ± 0.012		
AM94	SpSabS1+ ERG20	0.056 ± 0.018		
AM94	SpSabS1+ *Pa*IDS2	0.070 ± 0.008	1.40	1.40
AM94	SpSabS1+ Erg20p(A99C)	0.072 ± 0.021	1.29	1.41
AM94	SpSabS1+ ERG20(A99L)	0.081 ± 0.020	1.45	1.59
AM94	SpSabS1+ ERG20(A99F)	0.093 ± 0.019	1.66	1.82
AM94	SpSabS1+ ERG20(A99W)	0.105 ± 0.023	1.88	2.06
AM94	SpSabS1+ ERG20(F96W)	0.180 ± 0.020	3.21	3.53
AM94	SpSabS1+ Erg20p(N127W)	0.312 ± 0.024	5.57	6.12
AM94	SpSabS1+ Erg20p(F96W-N127W)	0.530 ± 0.050	1.70	10.39
AM94	Erg20p(F96W-N127W)-SpSabS1	1.870 ± 0.060	3.53	36.67
MIC2	Erg20p(F96W-N127W)-SpSabS1	12.900 ± 2.950	6.90	252.94
MIC2	2 × Erg20p(F96W-N127W)-SpSabS1	17.500 ± 2.065	1.35	343.13

Table 3. Steady-State Kinetic Parameters of Recombinant Wild-Type and Mutant Erg20p

Erg20p variant	K_M^{DMAPP} (μM)	k_{cat}^{DMAPP} (s^{-1})	K_M^{GPP} (μM)	k_{cat}^{GPP} (s^{-1})
wt	0.17 ± 0.08	0.025 ± 0.014	0.43 ± 0.07	0.061 ± 0.024
F96W	0.32 ± 0.19	0.011 ± 0.003	13.36 ± 2.97	0.024 ± 0.009
N127W	0.30 ± 0.08	0.010 ± 0.004	22.61 ± 3.51	0.011 ± 0.005
F96W-N127W	0.49 ± 0.26	0.012 ± 0.002	27.56 ± 4.91	0.021 ± 0.006

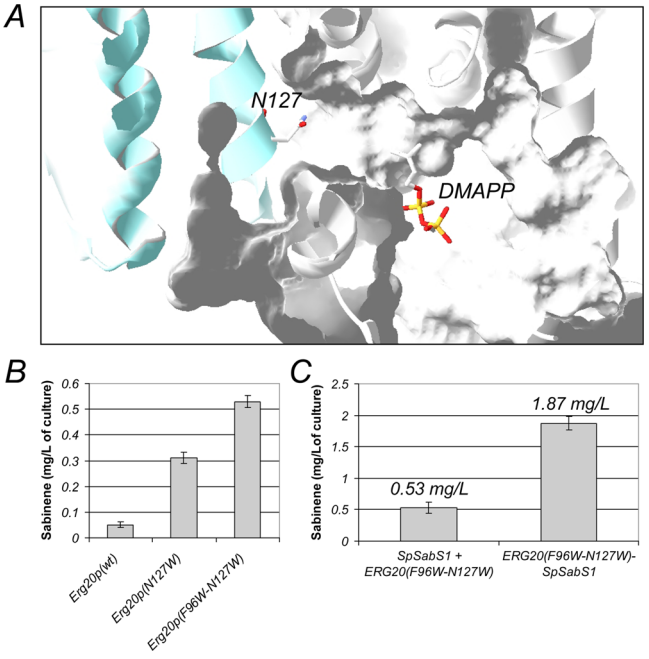

Figure 4. Engineering a dominant negative function into Erg20p. (A) Model of Erg20p showing the N127 residue proposed to form part of the active site of the other subunit of the Erg20p dimer. (B) Single Erg20p(N127W) and double Erg20p(F96W-N127W) mutants expressed from high copy number plasmids increase sabinene yield by 6- and 10.5-fold, respectively, compared with wild-type Erg20p. C. Fusion of *Sp*SabS1 with the double Erg20p(F96W-N127W) mutant through a 5xGS linker results in an additional increase of 3.5-fold.

homodimers of the wild type protein to support FPP synthesis. Indeed, the double mutant Erg20p(F96W-N127W) has a strong dominant negative function, increasing the yield of sabinene production by 10.4 fold to 0.53 mg/L (Figure 4B and Table 2). Determination of the steady state kinetic parameters of the reaction catalyzed by recombinant Erg20p(N127W) and Erg20p(F96W-N127W) variants *in vitro* confirmed that these mutants also exhibit significantly lower affinity for GPP than wild-type Erg20p, in agreement with the above findings (Table 3).

Erg20p Fusions. Analysis of the FOH and NOH levels in the cells expressing the double Erg20p mutant N127W-F96W revealed that despite the 10-fold increase in monoterpene production, the sesquiterpenol levels in the culture medium were only partly decreased (data not shown). This suggests that a significant amount of GPP is still preferably picked up by FPP synthesizing Erg20p subunits, despite their low abundance. This could be the case if the site of GPP production by Erg20p and that of GPP utilization by SpSabS1 are different. GPP would then be rapidly picked up by the few FPP synthesizing subunits, before diffusing to the rest of the cell. To overcome this potential limitation, we decided to fuse SpSabS1 to Erg20p, so as to direct it to the correct subcellular compartment and to enable it to rapidly sequester GPP at the site of its production. Fusion of the double mutant Erg20p(F96W-N127W) with SpSabS1 resulted in a 3.5-fold increase in sabinene yield, reaching 1.87 mg/L (Figure 4C and Table 2).

Screening Heterozygous Deletion Strains. Aiming to improve sesquiterpene production in yeast, we previously developed a set of AM94-derived strains carrying heterozygous deletions in genes that were identified as positive genetic interactors of *HMG2*. Tandem heterozygous deletion of three of these genes resulted in an 11-fold increase in caryophyllene yield.[16] We tested a selection of these strains, including AM97 (*ubc7/UBC7*), AM102(*ubc7/UBC7, ssm4/SSM4*), and AM109 (*ubc7/UBC7, ssm4/SSM4, pho86/PHO86*), to examine whether the same set of deletions also improved monoterpene production. All three strains exhibited similar yield to AM94 (data not shown), suggesting that genetic modifications that influence sesquiterpene production may not have an effect on monoterpene production or that the limiting factors in each system are distinct.

Heterozygous Deletion of the Phosphatase Genes *DPP1* and *LPP1*. It has recently been proposed that the yeast phosphatases Lpp1p and Dpp1p compete with sesquiterpene

dx.doi.org/10.1021/sb400115e | *ACS Synth. Biol.* 2014, 3, 298−306

synthases for the FPP substrate and deletion of either or both phosphatases has a beneficial effect in sesquiterpene production.[15] We constructed AM94 strain derivatives carrying heterozygous deletions of LPP1 and/or DPP1 (Table 1) and tested their contribution to sabinene production. A strong negative effect in yield was observed in both single mutants (*lpp1/LPP1* or *dpp1/DPP1*) and in the double mutant (*dpp1/DPP1*, *lpp1/LPP1*; data not shown). This negative effect of the deletions was also observed when the same strains were tested for sesqui- and diterpene production (data not shown). This discrepancy with the observations of Scalcinati and coworkers[15] may be related to the overall prenyl diphosphate levels present in the cells, as deletion of the phosphatases will result in even higher levels of prenyl diphosphates, which may function as strong negative feedback regulators of the mevalonate pathway.

Deletion of One *ERG20* Allele. Generally, deletion of one of the two copies of a gene in a diploid *S. cerevisiae* strain results in approximately 50% decrease in the levels of the corresponding protein.[29] To reduce the levels of wild-type Erg20p, we deleted one *ERG20* allele from AM94 cells giving rise to the *erg20/ERG20* heterozygous deletion strain MIC2. Overproduction of the Erg20p(F96W-N127W)-SabS1 fusion in MIC2 resulted in a 7-fold increase in production, reaching 12.9 mg/L (Table 2). To further increase product yield, we introduced a second plasmid vector producing the same fusion (pWTDH/Erg20p(F96W-N127W)-SabS1), and obtained an additional 35% increase reaching 17.5 mg/L sabinene (Table 2). Overall, the improvements described here achieve a 340-fold increase in sabinene yield from the 0.05 mg/L observed with the base strain AM94 (Table 2).

Conclusions. Previous efforts in monoterpene production in yeast achieved approximately 5 mg/L geraniol from a haploid strain that contains a mutant form of Erg20p (K197G), but the mutant yeast strain exhibits slower growth rates.[18] The design developed here overcomes a major hurdle in monoterpene production in yeast, that of the sequential nature of the yeast farnesyl diphosphate synthase reaction, without any obvious effects on the growth characteristics of the yeast strains examined.

Our findings also indicate that proper integration of heterologous enzymatic activities in the host's existing biosynthetic pathways may be a limiting factor affecting product yields, and that engineering synthetic components based on endogenous protein scaffolds may be an advantageous approach in Synthetic Biology efforts. The use of protein fusions or artificial scaffolds has greatly aided the efficient metabolic channeling in sesqui- and diterpene production in microorganisms.[30−33] Taking advantage of the ability of Erg20p to dimerize, the synthetic Erg20p fusion components developed here can act as a scaffold for the assembly of larger metabolic complexes.

Several studies have reported important progress in yeast strain improvement, applying approaches ranging from classic molecular genetics to systems biology (e.g.,[11] and others discussed in[19,34,35]). The synthetic part (dominant negative GPP synthase-terpene synthase fusion) can be incorporated to any such strain to further improve monoterpene yields, while the developed yeast strain (MIC2) and plasmid vectors can be used as a plug-and-play system for monoterpene synthase or downstream enzyme characterization, monoterpene pathway elucidation or product structural determination.

MATERIALS AND METHODS

Chemicals and Enzymes. 1,8 cineole (Aldrich, C8,060-1), γ-terpinene (Aldrich, T2134), α-pinene (Aldrich, P-7408), β-myrcene (M-0382), (−)-trans-caryophyllene (Sigma, C9653-5), *trans*-nerolidol (Fluka, 18143), linalool (Fluka, 51782), and a 70% sabinene solution kindly donated by VIORYL S.A., were used as standards. Phusion High-Fidelity DNA Polymerase (New England BioLabs, M0530S) and MyTaq DNA polymerase (BIO-21105, Bioline) were used in PCR amplifications. Substrates for the in vitro enzymatic reactions (DMAPP (D4287), IPP (I0503) and GPP (G6772) were all from Sigma. All restriction enzymes were from New England BioLabs. NucleoSpin Plasmid Kit (740588.250, Macherey-Nagel) was used for plasmid DNA purification. QIAquick Gel Extraction Kit (#28704, Qiagen) was used for gel extraction and DNA purification.

Yeast Media. D-(+)-Glucose monohydrate (16301, Sigma); D-(+)-galactose (G0625, Sigma); raffinose pentahydrate (R1030, US Biological); yeast nitrogen base w/o AA (Y2025, US Biologicals); complete minimal (CM) medium is composed of 0.13% (w/v) dropout powder (all essential amino acids), 0.67% (w/v) yeast nitrogen base w/o AA, 2% glucose. For galactose-based medium, glucose is substituted with 2% galactose, 1% raffinose.

Gene Cloning and Expression in Yeast. The following expression plasmids were used for expression in yeast cells: pYES2 (*URA3*, 2 μ, P_{Gal1}); pYES2myc (*URA3*, 2 μ, P_{Gal1}, myc tag); pWTDH3 (*TRP1*, 2 μ, P_{TDH3}); pWTDH3myc (*TRP1*, 2 μ, P_{TDH3}, myc tag); pUTDH3 (*URA3*, 2 μ, P_{TDH3}); pUTDH3myc (*URA3*, 2 μ, P_{TDH3}, myc tag); pHTDH3 (*HIS3*, 2 μ, P_{TDH3}); pHTDH3myc (*HIS3*, 2 μ, P_{TDH3}, myc tag). To generate the pYES2myc-GS(5) and pUTDH3m/GS(5) vectors, the complementary primers 5′GS(5): 5′-GAT CCT ATG TCG ACG GTA GCG GCA GCG GTA GCG GTA GCG GCA GCG AAT TCT ATC-3′ and 3′GS(5) 5′-TCG AGA TAG AAT TCG CTG CCG CTA CCG CTA CCG CTG CCG CTA CCG TCG ACA TAG-3′ were self-annealed and ligated into the pYES2myc and pUTDH3myc vectors digested with *Bam*HI and XhoI. Integration of the linker was confirmed by sequencing.

Constructs pYES2-IDI, pYES2-*PaIDS2* (*Pa*GPPS), and pUTDH/*Sf*CarS1 (described as pUTDH/*Sf*126) were previously described.[16,24]

The gene for the *S. pomifera*, sabinene synthase (*Sp*Sabs1) was isolated through an EST sequencing approach using a tissue-specific glandular trichome-derived cDNA library.[21] For expression in *S. cerevisiae*, the open reading frame of *Sp*SabS1 was amplified using primers 5SpSabS1-*Eco*RI 5′-GAA TTC ATG CGA CGC TCT GGG GAT TAC CA-3′ and 3SpSabS1-XhoI 5′-CTC GAG TCA GAC ATA AGG CTG GAA TAG CA-3′, removing the chloroplastic transit peptide, and introduced into pCRII-TOPO (Invitrogen) by TOPO TA cloning. The SabS1 ORF from pCRII-TOPO was digested with *Eco*RI and *Xho*I enzymes and transferred into pYES2myc, pJG4-4, pHTDH3, and pYES2myc/ERG20-GS(5) vectors. The ERG20-GS-*Sp*Sabs1 insert of pYES2myc/ERG20-GS-SpSabS1 was digested with *Bam*HI and *Xho*I and subcloned into the pWTDH3myc vector.

For the construction of pUTDH3/ERG20, the ERG20 ORF was amplified from yeast genomic DNA with 5ERG20-*Eco*RI 5′-GAA TTC ATG GCT TCA GAA AAA GAA ATT AG-3′ and 3ERG20-XhoI 5′-CTC GAG CTA TTT GCT TCT CTT

dx.doi.org/10.1021/sb400115e | *ACS Synth. Biol.* 2014, 3, 298−306

GTA AAC-3′ primers and cloned into pCRII-TOPO. The insert was subcloned into the *Eco*RI and XhoI restriction sites of pUTDH3 and pYES/GS(5) vectors. Insertion of ERG20 in the latter brings the gene in-frame to a five Gly-Ser repeat (indicated as GS(5)) used as a flexible linker between the two fused polypeptides. For the construction of pYES2/ERG20-GS, the ERG20 ORF was amplified using 5ERG20-*Bam*HII 5′-GGA TCC ATG GCT TCA GAA AAA GAA ATT AG-3′ and 3ERG20-XhoI-nostop 5′-CTC GAG TTT GCT TCT CTT GTA AAC-3′ primers and inserted into *Bam*HI and *Sal*I digested pYES2myc/GS(5) vector.

The bacterial expression constructs pRSETa-Erg20p, pRSETa-Erg20p(F96W), pRSETa-Erg20p(N127W), and pRSETa-Erg20p(F96W-N127W) were constructed by subcloning of the *Eco*RI/*Xho*I excised inserts of the corresponding pUTDH3/ERG20 wild-type and mutant plasmids into the bacterial expression vector pRSETa (Invitrogen).

Yeast Two-Hybrid. The ERG20 insert cloned into the pUTDH/ERG20 vector was digested with *Eco*RI and *Xho*I and subcloned into the pGILDA and pJG4-5 vectors linearized with the same restriction enzymes. The composite constructs fuse in frame the ERG20 protein with the LexA moiety of the pGILDA vector and the B42AD activation domain of the pJG4−5 vector. Interaction of two ERG20 monomers was assessed as previously described.[36]

Mutagenesis. Site-directed mutagenesis of ERG20 was performed with the Quickchange method (Stratagene) using primers: ERG20-F96W 5′-TGA GTT GTT GCA GGC TTA CTG GTT GGT CGC CGA TGA TAT G-3′, ERG20-A99TKK 5′-CAG GCT TAC TTC TTG GTC TKK GAT GAT ATG ATG GAC AAG TC-3′ (degenerate F, L, C, W), and ERG20-N127W 5′-GTT GGG GAA ATT GCC ATC TGG GAC GCA TTC ATG TTA GAG G-3′.

Development of Yeast Strains. To generate a deletion in one of the two alleles of the diploid yeast strain AM94, the protocol previously described in ref 24 was used. To generate strain MIC2 (Table 1), PCR amplification of the pUG27 cassette containing *his5+* from *S. pombe* flanked by loxP sites was performed using primers ERG20F 5′-GAG TCT CGT GGC TTC AAA GC-3′ and ERG20OL3 5′-TCT CGT ACT ACC CGT AAT TTC CGA TCA CGC ATT TCT TCAT TTT CAT TGG CGC ATA GGC CAC TAG TGG ATC TG-3′ which incorporate flanking sequences complementary to the 5′ and 3′ end of the *ERG20* gene respectively. Heterozygous deletions of *LPP1* were prepared by amplifying the pUG27 cassette using primers LPP1-600-pUGF 5′-GTT TGA GAT TTA TTG TTG GCA ACT TTC TTA CAT TTT TGT TGT TTC AAC TTC CAG CTG AAG CTT CGT ACG C-3′ and LPP1-2230-pUGR 5′-TCA AGA TCT CCT TGC ATA TGA AGA TTT GAC GTC GTT TAC AAG AGC TAT CTC AGA GCA TAG GCC ACT AGT GGA TCT G-3′. The PCR product was transformed into AM109 or AM112 cells, to derive strains AM111 and AM118, respectively (Table 1). To validate integration at the *lpp1* locus, PCR reactions were performed on colony genomic DNA using primers LPP1prom 5′-TTG TCC ATA TTC CTC GAT CCA CAC TTT CA-3′ and LPP1-2230-pUGR. Positive colonies were selected and transformed with pb227Gal-Cre vector expressing Cre recombinase to excise the *HIS3* selection marker. Heterozygous deletions of *DPP1* were prepared as above using primers DPP1-630-F 5′-TGC AGC ACG CCT GGC GTA TAC TGC TAT AAT TGT ACA TCA TGT TAT CGG CGT TGA CAG CTG AAG CTT CGT ACG C-3′ and DPP1-2061-R 5′-TAA ACT TCT AAG GCT TTC GTG TAA AGT GAT GTT GGG ATT GTC CGA TGA AAT AAC AAG GCA TAG GCC ACT AGT GGA TCT G-3′. Integration at dpp1 locus was validated using DPP1prom 5′-CAG ATA GTA CCT TTC AGG TGG TTA GAG-3′ and DPP1-2061-R.

Terpene Quantification and Extraction from Yeast Cells. Selected *S. cerevisiae* strains were cultivated in 10 mL liquid media. Quantification of terpene yield was done by dodecane overlay as described in,[37] followed by GC-FID analysis of 1 μL of the dodecane phase (chromatographic conditions were as described in[21]). Sabinene quantification was carried out by comparison with pure standard, provided by VIORYL S.A., Athens, Greece. When necessary, terpene extraction was performed using 1% (w/v) Diaion HP20 (Supelco, Bellefonte, PA) as adsorbent resin following the protocol previously described.[16]

Determination of FPP. 50 mL cultures of the selected strains were grown to saturation and the cells were harvested by centrifugation at 3,000 rpm and washed twice with 10 mL H_2O. Yeast cells were resuspended in 1 mL of H_2O and disrupted by glass beads. After centrifugation at 13 000 for 10 min in a microfuge, 0.5 mL of the supernatant was mixed with 0.5 mL 2 N HCl in 83% ethanol and overlaid with 1 mL of hexane. The reactions were incubated at 37 °C for 10 min to hydrolyze the acid-labile diphosphates and subsequently neutralized by adding 0.35 mL of 10% NaOH. The mixtures were extracted by vortexing and the hexane phase was analyzed by GC-MS using the temperature program described in ref 21. Parallel samples incubated with HP-20 beads were used for the evaluation of terpenol content in the medium.

Protein Expression in Bacteria. Wild-type and mutant forms of 6xHis-tagged Erg20p was purified by Ni^{2+}-NTA affinity chromatography from 200 mL cultures of *E. coli* BL21 growing at 19 °C, according to the method described in ref 21.

Determination of Kinetic Parameters. Prenyl diphosphate synthase activities were assayed in a 0.2-mL reaction containing 10 mM MOPS (pH 7.0), 5 mM $MgCl_2$, 1 mM DTT, 0.1 mg/mL BSA, 0.01 mM IPP, and 50 ng of recombinant Erg20p (wild-type or mutant). Varying concentrations of DMAPP or GPP were added as substrates. Reactions were carried out for 30 min at 30 °C; and then, they were terminated by the addition of 0.2 mL 2N HCl in 83% ethanol and overlaid with 0.1 mL hexane to trap the volatile products. After 10 min at 37 °C to hydrolyze the acid-labile diphosphates (as above), reactions were neutralized by adding 0.35 mL of 10% NaOH. The hexane phase (2 μL) was analyzed by GC-MS, using the conditions described in ref 21. The experiments were carried out in duplicate.

Construction of the Erg20p Model. The structural model of Erg20p was constructed using the SWISS-MODEL server in automated mode.[38−40]

■ ASSOCIATED CONTENT

Ⓢ Supporting Information

Figure S1: Comparison of relative FPP and sesquiterpenol levels in AM94 cells. Figures S2: Terpenol ratio in AM94 yeast cells. Figure S3: Confirmation of Erg20p dimerization by the yeast two-hybrid system. This material is available free of charge via the Internet at http://pubs.acs.org.

■ AUTHOR INFORMATION

Corresponding Author

*E-mail: s.kampranis@med.uoc.gr.

Notes

The authors declare no competing financial interest.

■ ACKNOWLEDGMENTS

We would like to sincerely thank Sofia Loupassaki for assistance with GC-MS analysis, Aglaia Michelaki for critically reading the manuscript, and Jean Masai for valuable comments. The initial *Pa*IDS2 construct was a kind gift of Prof. Jonathan Gershenzon (Max Planck Institute for Chemical Ecology, Jena, Germany). We thank Nikitas Ragoussis and Dimitris Georganakis of VIORYL S.A. (Athens, Greece) for providing monoterpene standards. This work was funded in part by a Greek Secretariat of Research and Technology grant (09SYN-879) that is cofinanced by the European Regional Development Fund.

■ ABBREVIATIONS

geranyl diphosphate, GPP; dimethylallyl diphosphate, DMAPP; isopentenyl diphosphate, IPP; farnesyl diphosphate, FPP; nerolidol, NOH; farnesol, FOH; geraniol, GOH; linalool, LOH; *Salvia pomifera* sabinene synthase, SpSabS1; *Salvia fruticosa* caryophyllene synthase, SfCarS1; *Picea abies* GPP synthase, PaIDS2; *Gallus gallus* FPP synthase, FPS1

■ REFERENCES

(1) Renninger, N. S., Ryder, J. A., and Fisher, K. J. S. (2008) Jet Fuel Compositions and Methods of Making and Using Same. WO 2008/140492 A2.

(2) Ryder, J. A. (2009) Jet Fuel Compositions. WO 2010/033183 A2.

(3) Photo Release: Azul Brazilian Airlines Makes Successful Demonstration Flight with Amyris Renewable Jet Fuel Produced from Sugarcane. http://www.globenewswire.com/news-release/2012/06/19/479691/259556/en/Photo-Release-Azul-Brazilian-Airlines-Makes-Successful-Demonstration-Flight-With-Amyris-Renewable-Jet-Fuel-Produced-From-Sugarcane.html (accessed Jan 3, 2014).

(4) McGarvey, D. J., and Croteau, R. (1995) Terpenoid metabolism. *Plant Cell 7*, 1015−26.

(5) Anderson, M. S., Yarger, J. G., Burck, C. L., and Poulter, C. D. (1989) Farnesyl diphosphate synthetase. Molecular cloning, sequence, and expression of an essential gene from Saccharomyces cerevisiae. *J. Biol. Chem. 264*, 19176−84.

(6) Chambon, C., Ladeveze, V., Oulmouden, A., Servouse, M., and Karst, F. (1990) Isolation and properties of yeast mutants affected in farnesyl diphosphate synthetase. *Curr. Genet. 18*, 41−6.

(7) Kuranda, K., Grabinska, K., Berges, T., Karst, F., Leberre, V., Sokol, S., Francois, J., and Palamarczyk, G. (2009) The YTA7 gene is involved in the regulation of the isoprenoid pathway in the yeast *Saccharomyces cerevisiae*. *FEMS Yeast Res. 9*, 381−90.

(8) Hesselberth, J. R., Miller, J. P., Golob, A., Stajich, J. E., Michaud, G. A., and Fields, S. (2006) Comparative analysis of *Saccharomyces cerevisiae* WW domains and their interacting proteins. *Genome Biol. 7*, R30.

(9) Ho, Y., Gruhler, A., Heilbut, A., Bader, G. D., Moore, L., Adams, S. L., Millar, A., Taylor, P., Bennett, K., Boutilier, K., Yang, L., Wolting, C., Donaldson, I., Schandorff, S., Shewnarane, J., Vo, M., Taggart, J., Goudreault, M., Muskat, B., Alfarano, C., Dewar, D., Lin, Z., Michalickova, K., Willems, A. R., Sassi, H., Nielsen, P. A., Rasmussen, K. J., Andersen, J. R., Johansen, L. E., Hansen, L. H., Jespersen, H., Podtelejnikov, A., Nielsen, E., Crawford, J., Poulsen, V., Sorensen, B. D., Matthiesen, J., Hendrickson, R. C., Gleeson, F., Pawson, T., Moran, M. F., Durocher, D., Mann, M., Hogue, C. W., Figeys, D., and Tyers, M. (2002) Systematic identification of protein complexes in *Saccharomyces cerevisiae* by mass spectrometry. *Nature 415*, 180−3.

(10) Ro, D. K., Paradise, E. M., Ouellet, M., Fisher, K. J., Newman, K. L., Ndungu, J. M., Ho, K. A., Eachus, R. A., Ham, T. S., Kirby, J., Chang, M. C., Withers, S. T., Shiba, Y., Sarpong, R., and Keasling, J. D. (2006) Production of the antimalarial drug precursor artemisinic acid in engineered yeast. *Nature 440*, 940−3.

(11) Westfall, P. J., Pitera, D. J., Lenihan, J. R., Eng, D., Woolard, F. X., Regentin, R., Horning, T., Tsuruta, H., Melis, D. J., Owens, A., Fickes, S., Diola, D., Benjamin, K. R., Keasling, J. D., Leavell, M. D., McPhee, D. J., Renninger, N. S., Newman, J. D., and Paddon, C. J. (2012) Production of amorphadiene in yeast, and its conversion to dihydroartemisinic acid, precursor to the antimalarial agent artemisinin. *Proc. Natl. Acad. Sci. U.S.A. 109*, E111−8.

(12) Paddon, C. J., Westfall, P. J., Pitera, D. J., Benjamin, K., Fisher, K., McPhee, D., Leavell, M. D., Tai, A., Main, A., Eng, D., Polichuk, D. R., Teoh, K. H., Reed, D. W., Treynor, T., Lenihan, J., Fleck, M., Bajad, S., Dang, G., Dengrove, D., Diola, D., Dorin, G., Ellens, K. W., Fickes, S., Galazzo, J., Gaucher, S. P., Geistlinger, T., Henry, R., Hepp, M., Horning, T., Iqbal, T., Jiang, H., Kizer, L., Lieu, B., Melis, D., Moss, N., Regentin, R., Secrest, S., Tsuruta, H., Vazquez, R., Westblade, L. F., Xu, L., Yu, M., Zhang, Y., Zhao, L., Lievense, J., Covello, P. S., Keasling, J. D., Reiling, K. K., Renninger, N. S., and Newman, J. D. (2013) High-level semi-synthetic production of the potent antimalarial artemisinin. *Nature 496*, 528−32.

(13) Peralta-Yahya, P. P., Ouellet, M., Chan, R., Mukhopadhyay, A., Keasling, J. D., and Lee, T. S. (2012) Identification and microbial production of a terpene-based advanced biofuel. *Nat. Commun. 2*, 483.

(14) Nguyen, T. D., MacNevin, G., and Ro, D. K. (2012) *De novo* synthesis of high-value plant sesquiterpenoids in yeast. *Methods Enzymol 517*, 261−78.

(15) Scalcinati, G., Knuf, C., Partow, S., Chen, Y., Maury, J., Schalk, M., Daviet, L., Nielsen, J., and Siewers, V. (2012) Dynamic control of gene expression in *Saccharomyces cerevisiae* engineered for the production of plant sesquitepene α-santalene in a fed-batch mode. *Metab. Eng. 14*, 91−103.

(16) Ignea, C., Trikka, F. A., Kourtzelis, I., Argiriou, A., Kanellis, A. K., Kampranis, S. C., and Makris, A. M. (2012) Positive genetic interactors of HMG2 identify a new set of genetic perturbations for improving sesquiterpene production in *Saccharomyces cerevisiae*. *Microb. Cell Fact 11*, 162.

(17) Carrau, F. M., Medina, K., Boido, E., Farina, L., Gaggero, C., Dellacassa, E., Versini, G., and Henschke, P. A. (2005) *De novo* synthesis of monoterpenes by *Saccharomyces cerevisiae* wine yeasts. *FEMS Microbiol. Lett. 243*, 107−15.

(18) Fischer, M. J., Meyer, S., Claudel, P., Bergdoll, M., and Karst, F. (2011) Metabolic engineering of monoterpene synthesis in yeast. *Biotechnol. Bioeng. 108*, 1883−92.

(19) Kampranis, S. C., and Makris, A. M. (2012) Developing a yeast cell factory for the production of terpenoids. *Comput. Struct. Biotechnol. J. 3*, DOI: 10.5936/csbj.201210006.

(20) Austin, M. B., O'Maille, P. E., and Noel, J. P. (2008) Evolving biosynthetic tangos negotiate mechanistic landscapes. *Nat. Chem. Biol. 4*, 217−22.

(21) Kampranis, S. C., Ioannidis, D., Purvis, A., Mahrez, W., Ninga, E., Katerelos, N. A., Anssour, S., Dunwell, J. M., Degenhardt, J., Makris, A. M., Goodenough, P. W., and Johnson, C. B. (2007) Rational conversion of substrate and product specificity in a salvia monoterpene synthase: Structural insights into the evolution of terpene synthase function. *Plant Cell 19*, 1994−2005.

(22) Faulkner, A., Chen, X., Rush, J., Horazdovsky, B., Waechter, C. J., Carman, G. M., and Sternweis, P. C. (1999) The LPP1 and DPP1 gene products account for most of the isoprenoid phosphate phosphatase activities in *Saccharomyces cerevisiae*. *J. Biol. Chem. 274*, 14831−7.

(23) Goodman, D. S., and Popjak, G. (1960) Studies on the biosynthesis of cholesterol. XII. Synthesis of allyl pyrophosphates from mevalonate and their conversion into squalene with liver enzymes. *J. Lipid Res. 1*, 286−300.

(24) Ignea, C., Cvetkovic, I., Loupassaki, S., Kefalas, P., Johnson, C. B., Kampranis, S. C., and Makris, A. M. (2011) Improving yeast strains using recyclable integration cassettes, for the production of plant terpenoids. *Microb. Cell Fact. 10*, 4.

(25) Schmidt, A., and Gershenzon, J. (2008) Cloning and characterization of two different types of geranyl diphosphate synthases from Norway spruce (*Picea abies*). *Phytochemistry 69*, 49−57.
(26) Tarshis, L. C., Proteau, P. J., Kellogg, B. A., Sacchettini, J. C., and Poulter, C. D. (1996) Regulation of product chain length by isoprenyl diphosphate synthases. *Proc. Natl. Acad. Sci. U.S.A. 93*, 15018−23.
(27) Stanley Fernandez, S. M., Kellogg, B. A., and Poulter, C. D. (2000) Farnesyl diphosphate synthase. Altering the catalytic site to select for geranyl diphosphate activity. *Biochemistry 39*, 15316−21.
(28) Tarshis, L. C., Yan, M., Poulter, C. D., and Sacchettini, J. C. (1994) Crystal structure of recombinant farnesyl diphosphate synthase at 2.6-A resolution. *Biochemistry 33*, 10871−7.
(29) Springer, M., Weissman, J. S., and Kirschner, M. W. (2010) A general lack of compensation for gene dosage in yeast. *Mol. Syst. Biol. 6*, 368.
(30) Albertsen, L., Chen, Y., Bach, L. S., Rattleff, S., Maury, J., Brix, S., Nielsen, J., and Mortensen, U. H. (2011) Diversion of flux toward sesquiterpene production in *Saccharomyces cerevisiae* by fusion of host and heterologous enzymes. *Appl. Environ. Microbiol. 77*, 1033−40.
(31) Ohto, C., Muramatsu, M., Obata, S., Sakuradani, E., and Shimizu, S. (2010) Production of geranylgeraniol on overexpression of a prenyl diphosphate synthase fusion gene in Saccharomyces cerevisiae. *Appl. Microbiol. Biotechnol. 87*, 1327−34.
(32) Tokuhiro, K., Muramatsu, M., Ohto, C., Kawaguchi, T., Obata, S., Muramoto, N., Hirai, M., Takahashi, H., Kondo, A., Sakuradani, E., and Shimizu, S. (2009) Overproduction of geranylgeraniol by metabolically engineered *Saccharomyces cerevisiae*. *Appl. Environ. Microbiol. 75*, 5536−43.
(33) Zhou, Y. J., Gao, W., Rong, Q., Jin, G., Chu, H., Liu, W., Yang, W., Zhu, Z., Li, G., Zhu, G., Huang, L., and Zhao, Z. K. (2012) Modular pathway engineering of diterpenoid synthases and the mevalonic acid pathway for miltiradiene production. *J. Am. Chem. Soc. 134*, 3234−41.
(34) Kirby, J., and Keasling, J. D. (2009) Biosynthesis of plant isoprenoids: Perspectives for microbial engineering. *Annu. Rev. Plant Biol. 60*, 335−55.
(35) Krivoruchko, A., Siewers, V., and Nielsen, J. (2011) Opportunities for yeast metabolic engineering: Lessons from synthetic biology. *Biotechnol J 6*, 262−76.
(36) Kilili, K. G., Atanassova, N., Vardanyan, A., Clatot, N., Al-Sabarna, K., Kanellopoulos, P. N., Makris, A. M., and Kampranis, S. C. (2004) Differential roles of tau class glutathione S-transferases in oxidative stress. *J. Biol. Chem. 279*, 24540−51.
(37) Asadollahi, M. A., Maury, J., Moller, K., Nielsen, K. F., Schalk, M., Clark, A., and Nielsen, J. (2008) Production of plant sesquiterpenes in *Saccharomyces cerevisiae*: Effect of ERG9 repression on sesquiterpene biosynthesis. *Biotechnol. Bioeng. 99*, 666−77.
(38) Arnold, K., Bordoli, L., Kopp, J., and Schwede, T. (2006) The SWISS-MODEL workspace: A web-based environment for protein structure homology modelling. *Bioinformatics 22*, 195−201.
(39) Kiefer, F., Arnold, K., Kunzli, M., Bordoli, L., and Schwede, T. (2009) The SWISS-MODEL repository and associated resources. *Nucleic Acids Res. 37*, D387−92.
(40) Peitsch, M. C. (1996) ProMod and Swiss-Model: Internet-based tools for automated comparative protein modelling. *Biochem. Soc. Trans. 24*, 274−9.